

Determination of Hydrocarbon Potentials Using High Resolution Aeromagnetic Data over Sokoto Basin, Northwestern Nigeria

Ezekiel Kamureyina

Department of Geology and Mining, Adamawa State University, Mubi, Nigeria
Email: ezekielkamureyina@yahoo.com

How to cite this paper: Kamureyina, E. (2019) Determination of Hydrocarbon Potentials Using High Resolution Aeromagnetic Data over Sokoto Basin, Northwestern Nigeria. *International Journal of Geosciences*, 10, 419-438.
<https://doi.org/10.4236/ijg.2019.104024>

Received: January 21, 2019

Accepted: April 21, 2019

Published: April 24, 2019

Copyright © 2019 by author(s) and Scientific Research Publishing Inc. This work is licensed under the Creative Commons Attribution International License (CC BY 4.0).

<http://creativecommons.org/licenses/by/4.0/>



Open Access

Abstract

Aeromagnetic method of exploration is famed for its suitability for locating buried magnetic ore bodies because of their magnetic susceptibility. This method has been used in the early stage of petroleum exploration to determine depth and major structures of crystalline Basement rocks underlying the sedimentary basin. In this study, high resolution aeromagnetic data were used to ascertain the viability for hosting hydrocarbon potentials of the study area which forms part of the Illumedden Basin (also known locally as the Sokoto embayment) of West Africa. This was largely carried out through Spectra analysis to determine sediment thickness. The results of the analysis of the aeromagnetic data show that, deeper magnetic source ranges from 0.41 km to 2.69 km, shallow magnetic sources from 0.17 km to 0.97 km. Areas with shallow sediment thickness could not allow the thermal maturation of the sediments, since temperature increase with depth and a depth of two kilometers and above has a temperature range of 60°C and above. Areas with sediment thickness of 1.5 km and above were delineated and considered as sub-basins and hence potential areas for hydrocarbon exploration.

Keywords

Hydrocarbon Potentials, High Resolution Aeromagnetic Data, Spectral Analysis, Sokoto Basin, Nigeria

1. Introduction

The present work determines the potentials of the study area for hydrocarbon, based on the high resolution digital aeromagnetic data over Sokoto basin, indi-

cating that the basin is characterized by shallow and deeper sediments thickness. Areas with shallow sediments thickness could not allow the thermal maturation of the sediments since temperature increase with depth and a depth of two kilometer and above has a temperature range of 60°C and above [1]. The determination of hydrocarbon potentials was carried out using statistical spectral method as a tool for determining depth to magnetic sources.

Most economic minerals, oil, gas, and groundwater lie concealed beneath the earth surface, thus hidden from direct view. The presence and magnitude of these resources can only be ascertained by geophysical investigations of the subsurface geologic structures in the area. If the area under investigation has no previous geological information and the primary aim of the study is to search for hydrocarbon deposits; the first question that must be answered, is whether the sedimentary basin is large enough and thick enough to justify any further investigations [2].

The aim of a magnetic survey is to investigate subsurface geology on the basis of magnetic anomalies in the Earth's magnetic field resulting from the magnetic properties of the underlying rocks [3]. Aside from the principal objective in assisting for mineral and groundwater development through improved geologic mapping, aeromagnetic surveys have traditionally been applied at the early stage of petroleum exploration to determine depth and major structures of Crystalline Basement rocks underlying the Sedimentary basin.

In this study, high resolution aeromagnetic data were used to ascertain the viability of the area for hydrocarbon. The possible occurrence of minerals, oil and gas in commercial quantities in the Sokoto basin has been a subject of controversy due to very scanty prospectivity data. Apart from the Niger Delta basin whose current production of petroleum is derived, Nigeria is blessed with other numerous Sedimentary basins comprising the Anambra, Bida, Sokoto, Borno (Chad) and Dahomey basins as well as the Benue trough which is made up of Lower, Middle and upper Benue troughs; these basins have structural and stratigraphical similarities with contiguous intracratonic rifted basins of Niger Republic, Chad Republic, Sudan, Uganda, Tanzania and Kenya where commercial oil accumulations have been discovered and currently been exploited [4].

The aim of this work is to analyze and interpret the high resolution aeromagnetic data over the study area: to determine the thickness of the sediments through Spectral analysis. The work is aimed at acquainting future researchers with the knowledge of the area and to shed more light on sediment thickness which is crucial to hydrocarbon generation in the study area.

The study area lies between longitudes 4°00'E and 6°00'E and latitudes 11°30'N and 13°30'N (Figure 1). The topographical map of Figure 1 was obtained from digital elevation model (DEM) [5], and covers an area of approximately 48,400 km². It is part of the Illummeden Basin of West Africa, locally known as the Sokoto embayment situated in northwestern Nigeria [6] and [7]. It consists predominantly of a gently undulating plain with an average elevation

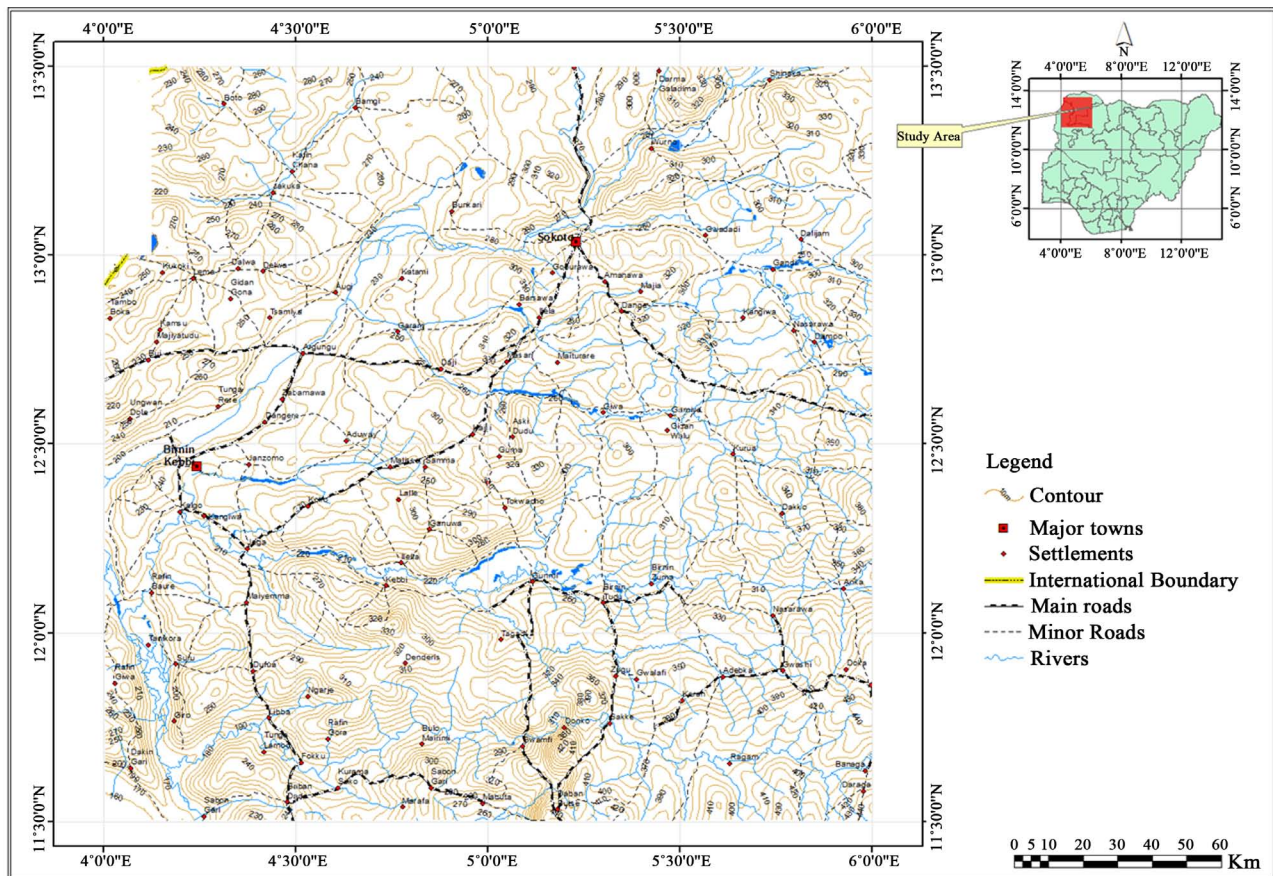


Figure 1. Topographic map of the study area [analyzed from Digital Elevation Model (DEM) 2006].

varying from 250 to 400 m above sea level. The plain is occasionally interrupted by low Mesas. A low Escarpment known as the “Dange Scarp” is the most prominent feature in the basin. The area to the east of the escarpment consists of mainly an undulating sandy plain, which extends south-westwards to the out-cropping basement complex [8].

The Sokoto basin falls within the hottest parts of Nigeria, belonging to the Sahel region of Africa. Temperatures are generally extreme, with average daily minimum of 16°C, during cool months of January and December, and the hottest months of April to June with an average maximum of 38°C and minimum of 24°C. Throughout the year average minimum temperature is 36°C and average daily minimum is 21°C. Rainfall is generally low with mean annual rainfall ranging from 600 mm to 1000 mm across the Basin. Much of the rain falls between the months of May to September, while the dry months are October to April [7].

The geology of Sokoto Basin is very well documented by several authors such as [4], [6], [8], [9] and [10]. According to [11], the geology of the study area (**Figure 2**) consists of Younger Basalts; Gwandu Formation; Sokoto group consisting of Gamba Formation, Kalambaina Formation and Dange Formation; Ri-ma group consisting of Wuruno Formation, Dukamaje Formation and Taloka Formation; Illo Formation, Gundumi Formation; Pan-African Younger Granitoids and Migmatite-Gneiss Complex.

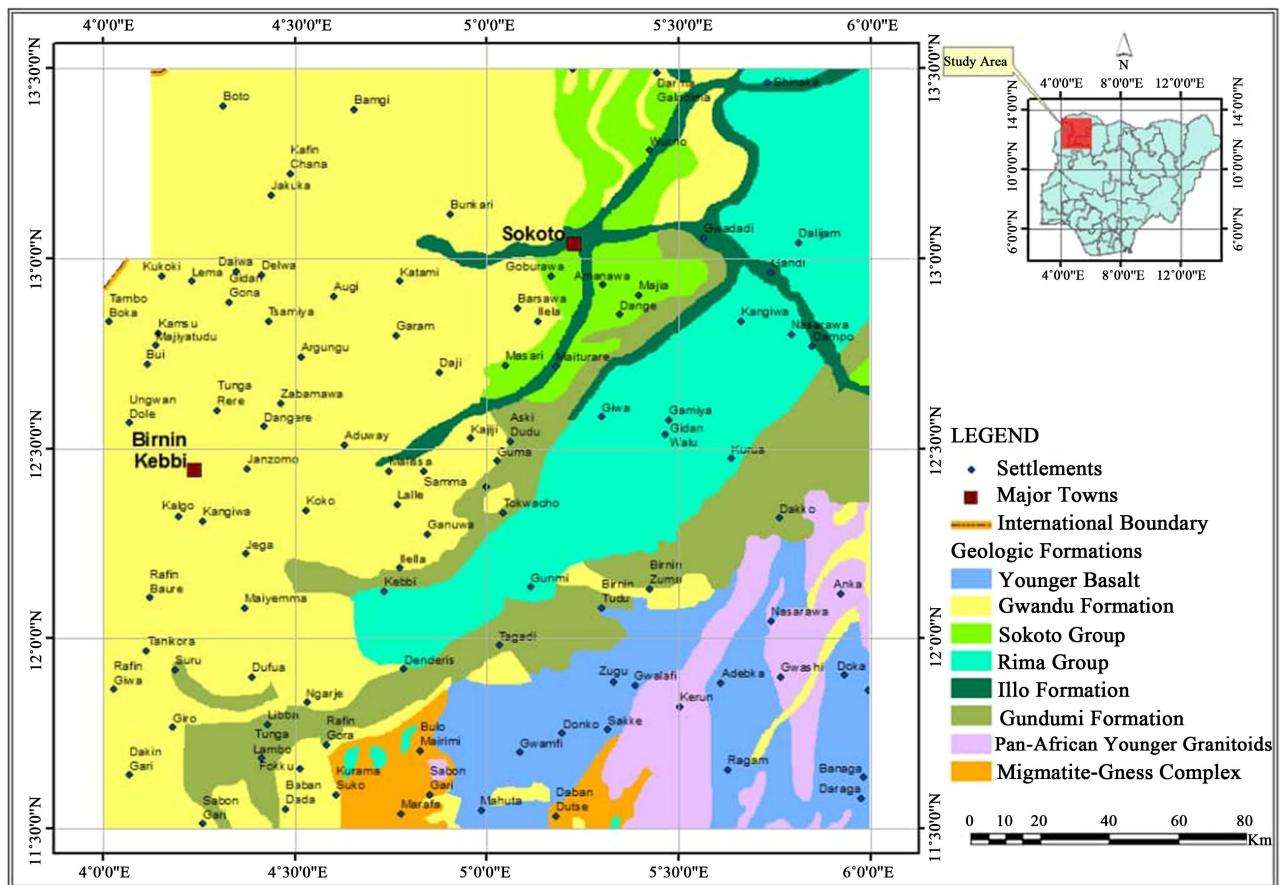


Figure 2. Geologic map of the study area (after Nigerian geologic survey agency, 2006).

The sediments of the Sokoto basin were accumulated during different phases of deposition. Overlying the Pre-Cambrian Basement unconformably, is the Illo and Gundumi Formations which are made up of grits and clays, constitute the Pre-Maastrichtian “Continental Intercalaire” of West Africa. They are overlain unconformably by the Maastrichtian Rima Group, consisting of Mudstones and friable Sandstones of Taloka and Wurno Formations separated by the fossiliferous, calcareous and shaley Dukamaje Formation. The Dange and the Gamba Formations which are mainly shales are separated by the calcareous Kalambaina Formation, which all constitute the Paleocene Sokoto Group. The overlying continental Gwandu Formation forms the Eocene Continental Terminal [4].

2. Materials and Methods

2.1. Data Acquisition

The high resolution aeromagnetic data that was used for the study consist of sixteen (16) sheets of aeromagnetic maps of total field intensity in half degree sheets obtained from Nigerian Geological Survey Agency (NGSA) [12]. The data was acquired by Fugro Airborne Survey Limited, as part of a programme aimed at assisting and promoting mineral exploration in Nigeria using 3× Scintrex CS3 Cesium Vapour Magnetometer with Flight Line Spacing of 500 meter, Flight

Line Direction NW-SE, Terrain Clearance 80 meters, Tie Line Spacing 2 kilometres.

2.2. Data Processing

Data was processed using various filters on the Aeromagnetic data which revealed certain features that aid the interpretation. Thus the digitized data was imported into the computer to produce the total Magnetic intensity maps. The Total Magnetic data was further subjected to Polynomial filtering to obtain both the Regional and the Residual maps. Spectral analysis was used to determine average sediment thickness. All these were carried out using the Oasis montaj, Math lab, and ArcGIS software.

In polynomial fitting the regional is matched with mathematical Polynomial of low order to expose the residual features as random errors, and the treatment is based on statistical theory. The observed data are used to compute, usually by least square method, the mathematically described surface given the closet fit to the magnetic field that can be obtained within a specified degree of detail. This surface is considered to be the regional field and the residual is the difference between the magnetic field values thus determined [13]. The simplest approach is to fit a polynomial of first order to the magnetic data over a large area as possible around the zone of interest and to subtract the polynomial surface from the observed surface. If the regional field were a simple inclined plane it will be a first order surface. Thus

$$Z = Ax + By + C \quad (1)$$

The next stage of complexity is the representation of a second order polynomial where,

$$Z = Ax^2 + By^2 + Cxy + Dx + Ey + F \quad (2)$$

The residual magnetic field of the study area was produced by subtracting the regional field from the total magnetic field using the Polynomial fitting method. The computer program aero-super map was used to generate the coordinates of the total intensity field data values. This super data file, for all the magnetic values was used for production of composite aeromagnetic map of the study area using Oasis Montaj software version 7.0.1 [14]. The program was used to derive the residual magnetic values by subtracting values of regional field from the total magnetic field values to produce the residual magnetic map and the regional map.

There are different methods that are used for depth calculation, such as the inversion methods based on Parker's forwarding calculation technique [15]. But the methods requires manual matching of anomalies to curve-types, which is time consuming and is restricted to the anomaly types for which curves exist, unlike the spectral method [16]. Developed a depth determination method which matches two dimensional power spectral calculated from gridded total magnetic intensity field data with corresponding spectral obtained from a theoretical model. For the purpose of analyzing aeromagnetic data, the ground is as-

sumed to consist of a number of independent ensembles of rectangular, vertical sided parallelepiped, and each is ensemble characterized by a joint frequency distribution for the depth (h) and length (b) and depth extent (t).

In this work, the characteristics of the residual magnetic field was studied using statistical spectral method. This was done by first transforming the data from space to the frequency domain and then analyzing their frequency characteristics. In the general case, the radial spectrum may be conveniently approximated by straight line segments, the slopes of which relate to depths of the possible layers, [16] and [17]. The residual total magnetic field intensity values are used to obtain the two dimensional Fourier Transform, from which the spectrum is to be extracted from the residual values $T(X, Y)$ consisting of M rows and N columns in $X - Y$. The evaluation is done using an algorithm that is a two dimensional extension of the fast Fourier transform [18]. Next, the frequency intervals are subdivided into sub-intervals, which lie within one unit of frequency range. The average spectrum of the partial values together constitutes the radial spectrum of the anomalous field [17], and [13].

The logarithm of the energy values versus frequency on a linear scale was plotted and the linear segments located the truncation effect (or Gibbs phenomenon). Three or two linear segments could be seen from the graphs. The first points on the frequency scale was ignored because the low frequency components in the energy spectrum are generated from the deepest layers whose locations are most likely in errors, each linear segment groups points due to anomalies caused by bodies occurring within a particular depth. If z is the mean depth of the layer, the depth factor for this ensemble of anomalies is $\exp(-2zk)$. Thus the logarithmic plot of the radial spectrum would give a straight line whose slope is $-2z$.

The mean depth of the burial ensemble is thus given as

$$Z = -\frac{m}{2} \quad (3)$$

where (m) is the slope of the best fitting straight line. Equation (3) can be applied directly if the frequency unit is in radian per kilometer. If however, the frequency unit is in circle per kilometer, the corresponding relationship can be expressed as

$$Z = -\frac{m}{4\pi} \quad (4)$$

In this study the aeromagnetic data set was divided into a block of $7.5' \times 7.5'$ ($13.73 \text{ km} \times 13.73 \text{ km}$) data points totaling 252 blocks excluding the Niger Republic part, which was subjected to Fast Fourier transformation (FFT) to compute the power spectrum of the magnetic data using Oasis montaj software.

3. Results and Discussion

3.1. Results

3.1.1. Total Magnetic Intensity Map

The total magnetic intensity map (Figure 3) of the study area was subdivided

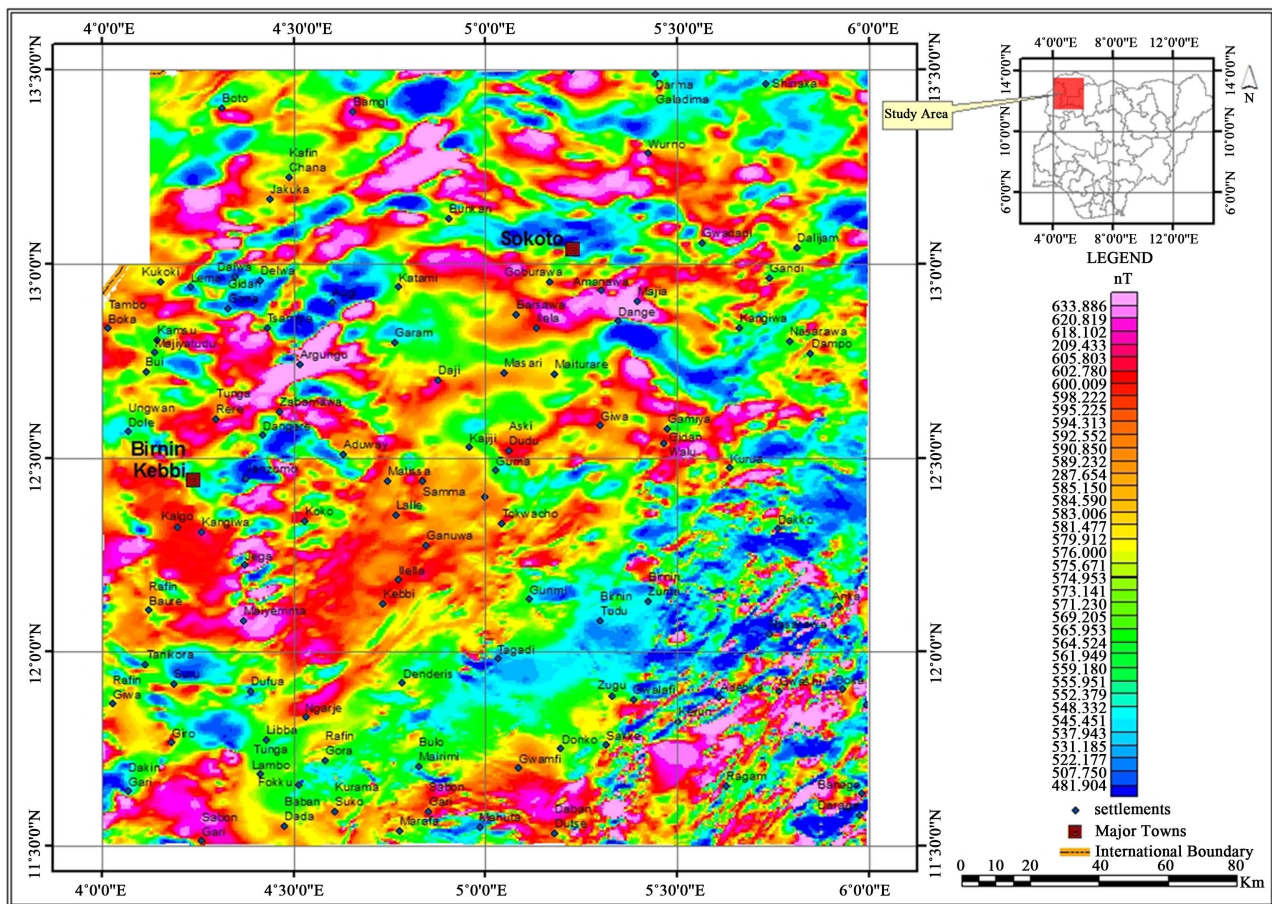


Figure 3. Total magnetic intensity map of the study area.

into three main sections: The northern part is characterized by low magnetic intensity values indicated by dark-light-blue-green-colour, while the eastern, western as well as the southern parts of the study area are characterized by low magnetic intensity values having dark-light-blue-green-colour dominating the area. The south western and south eastern parts of the study area are dominated by high magnetic intensity values, with pockets of reddish-pink colours disseminated in the northern part. Yellowish-orange-colours accompany the reddish-pink-colours depicting medium magnetic intensity values. The lowest total magnetic intensity value of the study area is 481.4 nT and highest value of 633.9 nT (Figure 3).

3.1.2. Residual Magnetic Intensity Map

The residual magnetic map (Figure 4), show magnetic anomalies with high magnetic intensity value of 59.6 nT and a low magnetic intensity value of -81.2 nT. The pink colour anomalies have magnetic intensity ranging from 34.6 nT to 59.6 nT which are prominent in the northern and eastern parts, with pockets in the southwestern part. Red colour anomalies vary from 13.3 nT to 30.7 nT and are dominant in the northern, central and southwestern parts, with pockets of disseminations in the south-eastern parts. Yellow colour anomalies range from

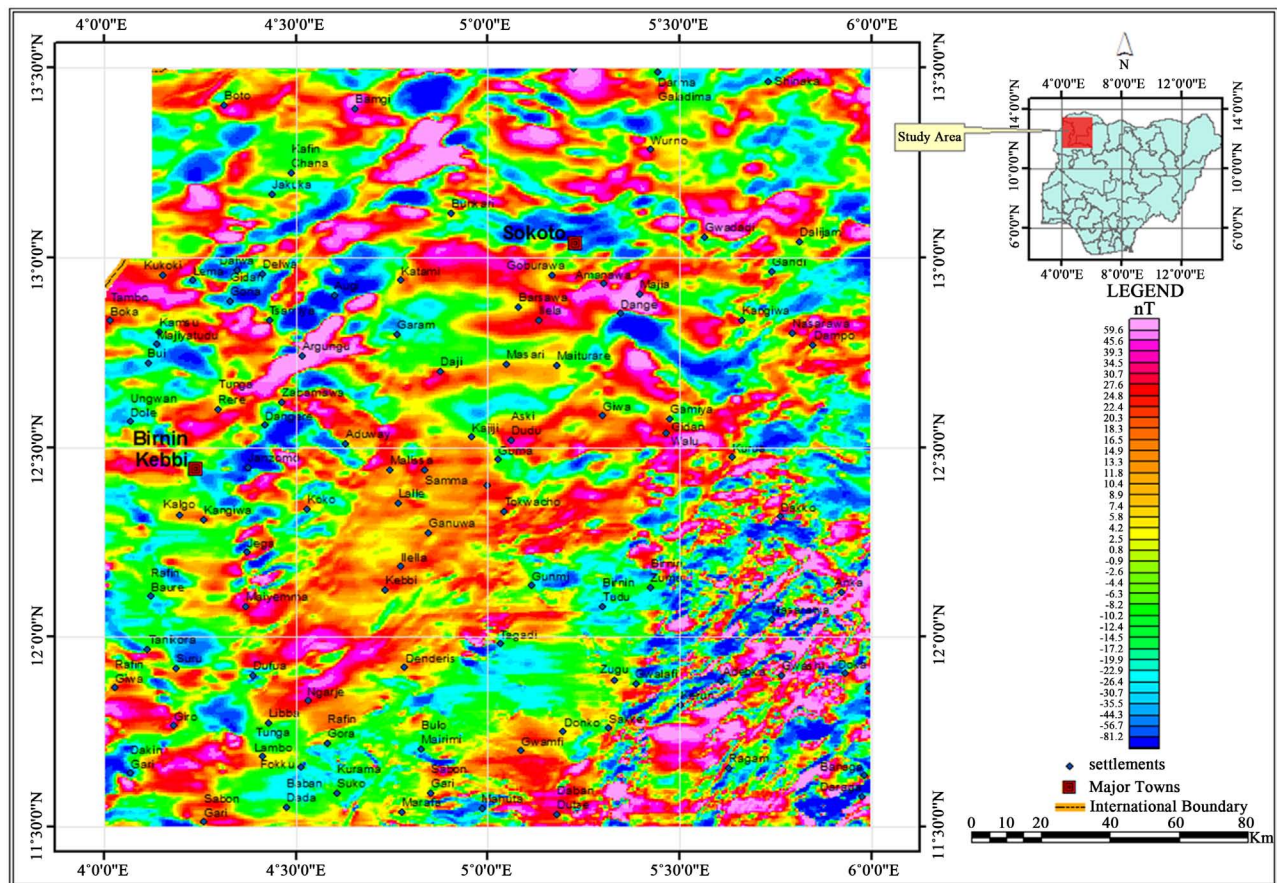


Figure 4. Residual magnetic intensity map of the study area.

2.5 nT to 11.8 nT and occur along the red colour anomalies, dominating the entire map. Green colour anomalies are found in the northern, southeastern, northeastern and south-western parts, with pockets of small occurrences in the south-south which varies from -17.2 nT to 0.8 nT. Blue colour anomalies range from -81.2 nT to -19.9 nT and are the most dominant, occurring in almost every part of the map. The residual magnetic map was divided into 252 blocks which were subjected into Fourier Transform, to obtain the radially average power spectrum (Figure 5).

3.1.3. Graphs of Spectral Analysis

The logarithm of spectral energies was plotted against obtained frequencies for the various blocks (Figure 6). The depth of the deeper magnetic sources (D1), and the depth to the shallow magnetic sources (D2) of that distribution from the slope of the second longest wave length segment was calculated. The deeper sources ranges from 0.41 km to 2.69 km, while the shallow sources ranges from 0.17 km to 0.97 km respectively. Table 1 shows the summary of the depths (D1 and D2). The results of D1 and D2 was contoured to produce contoured maps for D1 (Figure 7) and D2 (Figure 8) accompanied with coloured areas showing sub-basins that were identified in the study area. The contoured D1 was superimposed on the Geologic map of the study area (Figure 9).

Table 1. Summary of Deeper (D1) and Shallow (D2) Magnetic source depth obtained from spectral analysis of residual magnetic map of the study area.

Blocks	Deeper Sources (D1)	Shallow Sources (D2)
Block 1	1.48	0.17
Block 2	1.27	0.38
Block 3	1.38	0.21
Block 4	1.38	0.23
Block 5	2.03	0.30
Block 6	1.98	0.33
Block 7	1.51	0.31
Block 8	1.48	0.39
Block 9	1.13	0.19
Block 10	2.09	0.71
Block 11	1.32	0.32
Block 12	1.30	0.38
Block 13	1.24	0.30
Block 14	1.52	0.72
Block 15	1.27	0.45
Block 16	1.35	0.55
Block 17	1.95	0.77
Block 18	1.92	0.97
Block19	1.31	0.54
Block 20	1.24	0.36
Block 21	1.06	
Block 22	1.38	0.50
Block 23	1.23	0.24
Block 24	1.56	0.59
Block 25	1.11	0.35
Block 26	1.73	0.66
Block 27	1.35	0.44
Block 28	1.28	0.30
Block 29	1.16	0.46
Block 30	1.40	0.65
Block 31	1.28	0.40
Block 32	1.74	0.66
Block 33	1.39	0.53
Block 34	1.36	0.54
Block 35	1.43	0.52

Continued

Block 36	1.83	0.88
Block 37	1.09	0.46
Block 38	1.39	0.28
Block 39	1.20	0.35
Block 40	1.19	0.27
Block 41	1.31	0.52
Block 42	1.34	0.78
Block 43	1.38	0.78
Block 44	1.52	0.80
Block 45	1.68	0.71
Block 46	1.41	0.42
Block 47	1.17	0.46
Block 48	1.28	0.46
Block 49	1.37	0.50
Block 50	2.69	0.71
Block 51	1.43	0.82
Block 52	1.47	0.57
Block 53	1.67	0.74
Block 54	1.07	0.19
Block 55	1.20	0.27
Block 56	1.16	0.25
Block 57	1.20	0.46
Block 58	1.24	0.70
Block 59	1.11	0.58
Block 60	1.72	0.60
Block 61	1.64	0.75
Block 62	1.79	0.73
Block 63	1.21	0.26
Block 64	1.08	0.56
Block 65	1.15	0.51
Block 66	1.34	0.59
Block 67	1.60	0.66
Block 68	1.19	0.34
Block 69	1.58	0.56
Block 70	1.43	0.61
Block 71	1.07	0.29
Block 72	1.27	0.67

Continued

Block 73	1.39	0.49
Block 74	0.89	0.50
Block 75	1.10	0.67
Block 76	1.12	0.57
Block 77	1.41	0.60
Block 78	1.30	0.36
Block 79	1.26	0.61
Block 80	1.14	0.36
Block 81	1.38	0.61
Block 82	1.27	0.26
Block 83	1.74	0.64
Block 84	2.02	0.92
Block 85	1.71	0.71
Block 86	1.22	0.34
Block 87	1.76	0.84
Block 88	1.93	0.85
Block 89	2.41	0.90
Block 90	0.85	
Block 91	1.40	0.71
Block 92	2.26	0.72
Block 93	1.36	0.65
Block 94	1.37	0.74
Block 95	1.12	0.49
Block 96	1.07	0.35
Block 97	1.58	0.85
Block 98	1.14	0.61
Block 99	1.29	0.32
Block 100	1.79	0.88
Block 101	1.58	0.24
Block 102	1.34	0.69
Block 103	1.13	0.72
Block 104	1.27	0.58
Block 105	1.46	0.71
Block 106	1.44	0.72
Block 107	1.11	0.70
Block 108	1.20	0.60
Block 109	1.17	0.44
Block 110	1.35	0.77

Continued

Block 111	1.17	0.48
Block 112	1.28	0.48
Block 113	1.20	0.39
Block 114	1.24	0.50
Block 115	1.15	0.72
Block 116	1.67	0.78
Block 117	1.63	0.70
Block 118	1.61	0.76
Block 119	1.26	0.35
Block 120	1.16	0.50
Block 121	1.42	0.58
Block 122	0.95	0.50
Block 123	1.16	0.59
Block 124	0.76	0.41
Block 125	1.84	0.82
Block 126	1.36	0.37
Block 127	1.22	0.50
Block 128	1.34	0.52
Block 129	1.37	0.60
Block 130	1.30	0.57
Block 131	1.14	0.51
Block 132	0.17	0.25
Block 133	1.60	0.90
Block 134	1.23	0.43
Block 135	1.29	0.49
Block 136	1.21	0.59
Block 137	0.88	0.38
Block 138	1.27	0.62
Block 139	0.67	
Block 140	0.64	
Block 141	1.25	0.41
Block 142	2.05	0.72
Block 143	1.22	0.62
Block 144	1.14	0.68
Block 145	0.99	0.36
Block 146	1.13	0.55
Block 147	0.98	0.37

Continued

Block 148	0.72	
Block 149	0.75	
Block 150	0.96	0.55
Block 151	0.85	
Block 152	1.02	0.51
Block 153	0.90	0.42
Block 154	0.99	0.47
Block 155	0.52	
Block 156	1.37	0.46
Block 157	0.79	
Block 158	1.72	0.56
Block 159	1.02	0.47
Block 160	0.73	
Block 161	0.77	
Block 162	1.52	0.23
Block 163	1.29	0.64
Block 164	1.00	0.53
Block 165	1.09	0.53
Block 166	1.41	0.59
Block 167	0.79	0.31
Block 168	1.08	0.56
Block 169	0.65	0.39
Block 170	0.54	
Block 171	0.89	0.40
Block 172	0.86	0.41
Block 173	0.83	0.45
Block 174	1.37	0.69
Block 175	1.16	0.65
Block 176	1.19	0.56
Block 177	1.67	0.56
Block 178	1.21	0.60
Block 179	1.23	0.59
Block 180	1.18	0.38
Block 181	1.04	0.34
Block 182	1.19	0.51

Continued

Block 183	1.81	0.44
Block 184	0.62	0.33
Block 185	0.56	
Block 186	0.65	0.42
Block 187	0.49	
Block 188	0.51	
Block 189	1.06	0.44
Block 190	1.59	0.61
Block 191	1.15	0.49
Block 192	0.71	
Block 193	1.44	0.61
Block 194	1.21	0.59
Block 195	0.72	
Block 196	0.63	
Block 197	0.91	0.35
Block 198	1.26	0.66
Block 199	0.90	0.39
Block 200	0.77	0.49
Block 201	0.58	
Block 202	0.81	0.35
Block 203	1.03	0.46
Block 204	0.51	
Block 205	1.01	0.28
Block 206	1.18	0.56
Block 207	1.54	0.54
Block 208	1.70	0.38
Block 209	1.43	0.57
Block 210	0.64	
Block 211	1.12	0.5
Block 212	1.02	0.48
Block 213	1.70	0.32
Block 214	1.56	0.51
Block 215	0.64	
Block 216	0.62	
Block 217	0.52	

Continued

Block 218	0.79	0.39
Block 219	1.91	0.34
Block 220	0.87	0.45
Block 221	1.32	0.67
Block 222	1.13	0.48
Block 223	2.05	0.57
Block 224	2.60	0.60
Block 225	0.62	0.33
Block 226	0.52	
Block 227	0.57	
Block 228	0.62	
Block 229	1.04	0.41
Block 230	1.05	0.47
Block 231	0.56	
Block 232	0.41	
Block 233	0.58	
Block 234	1.19	0.45
Block 235	1.05	0.42
Block 236	0.81	0.48
Block 237	1.23	0.62
Block 238	1.12	0.46
Block 239	1.27	0.43
Block 240	1.63	0.45
Block 241	0.84	0.30
Block 242	0.44	
Block 243	0.49	
Block 244	0.85	0.41
Block 245	0.56	
Block 246	0.48	
Block 247	1.42	0.48
Block 248	1.02	0.43
Block 249	0.87	0.40
Block 250	1.43	0.46
Block 251	0.93	0.40
Block 252	0.54	

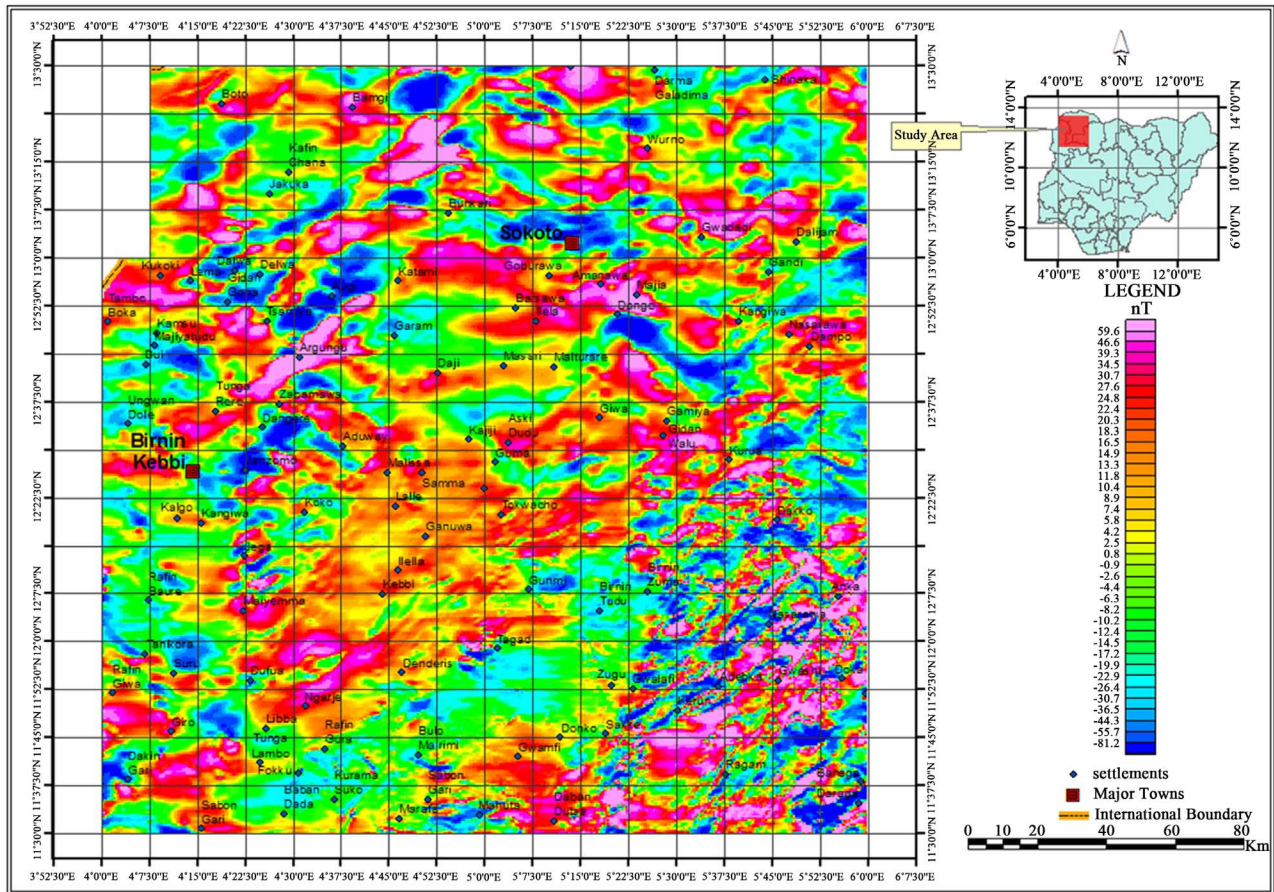


Figure 5. Gridded residual magnetic intensity map of Sokoto basin showing the 252 blocks that were subjected to fast fourier transformation to obtain the depth to magnetic source.

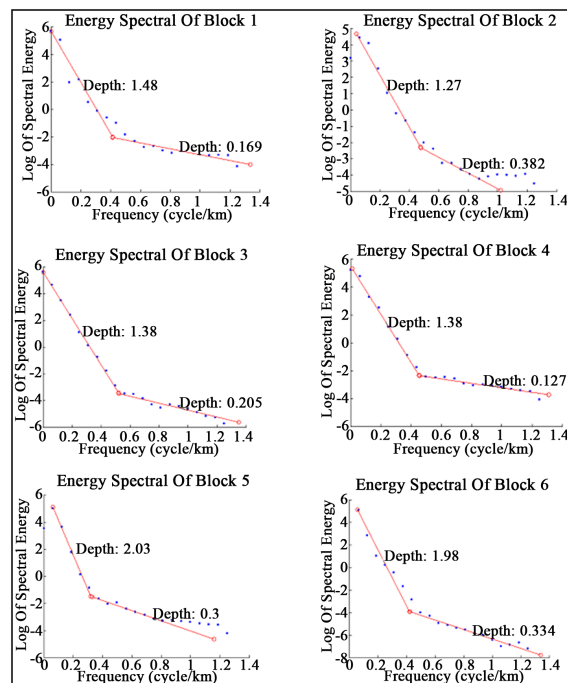


Figure 6. Examples of graphs of spectral blocks obtained in the study area.

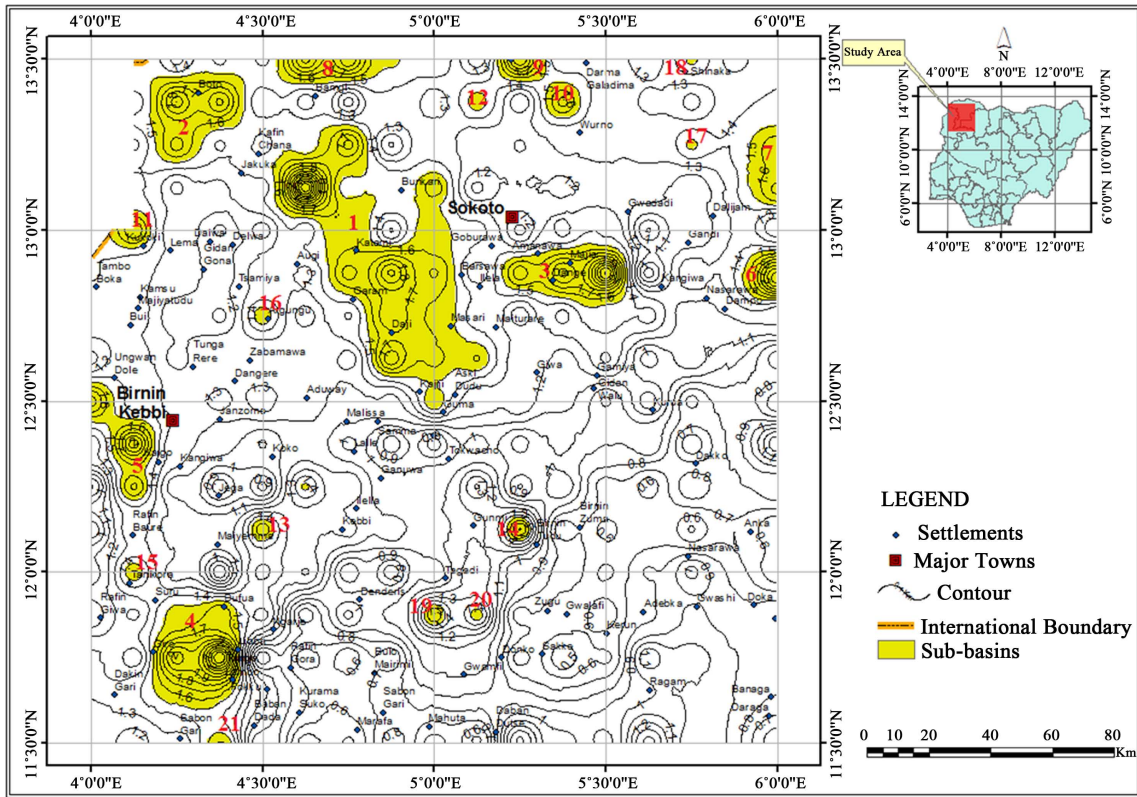


Figure 7. Magnetic source depths (deeper sources D1) contoured map of the study area (Cont. Int. 0.1 km).

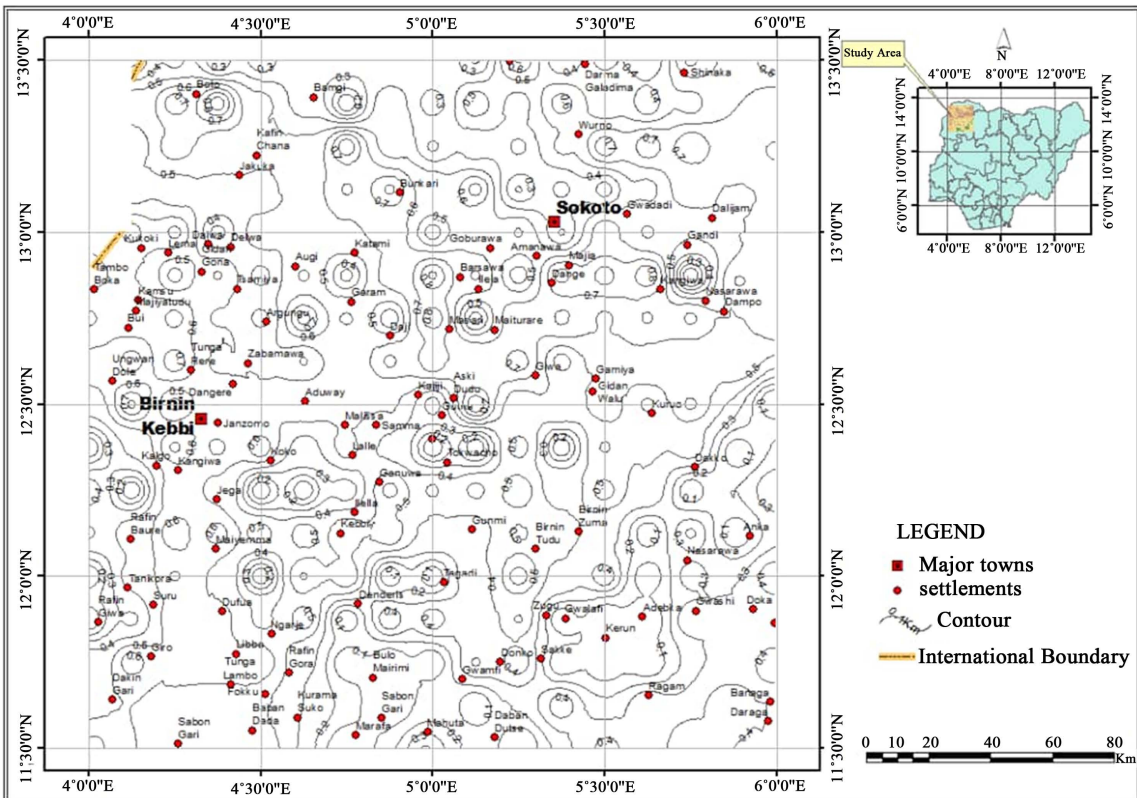


Figure 8. Magnetic source depths (shallow sources D2) contoured map of the study area (Cont. Int. 0.1 km).

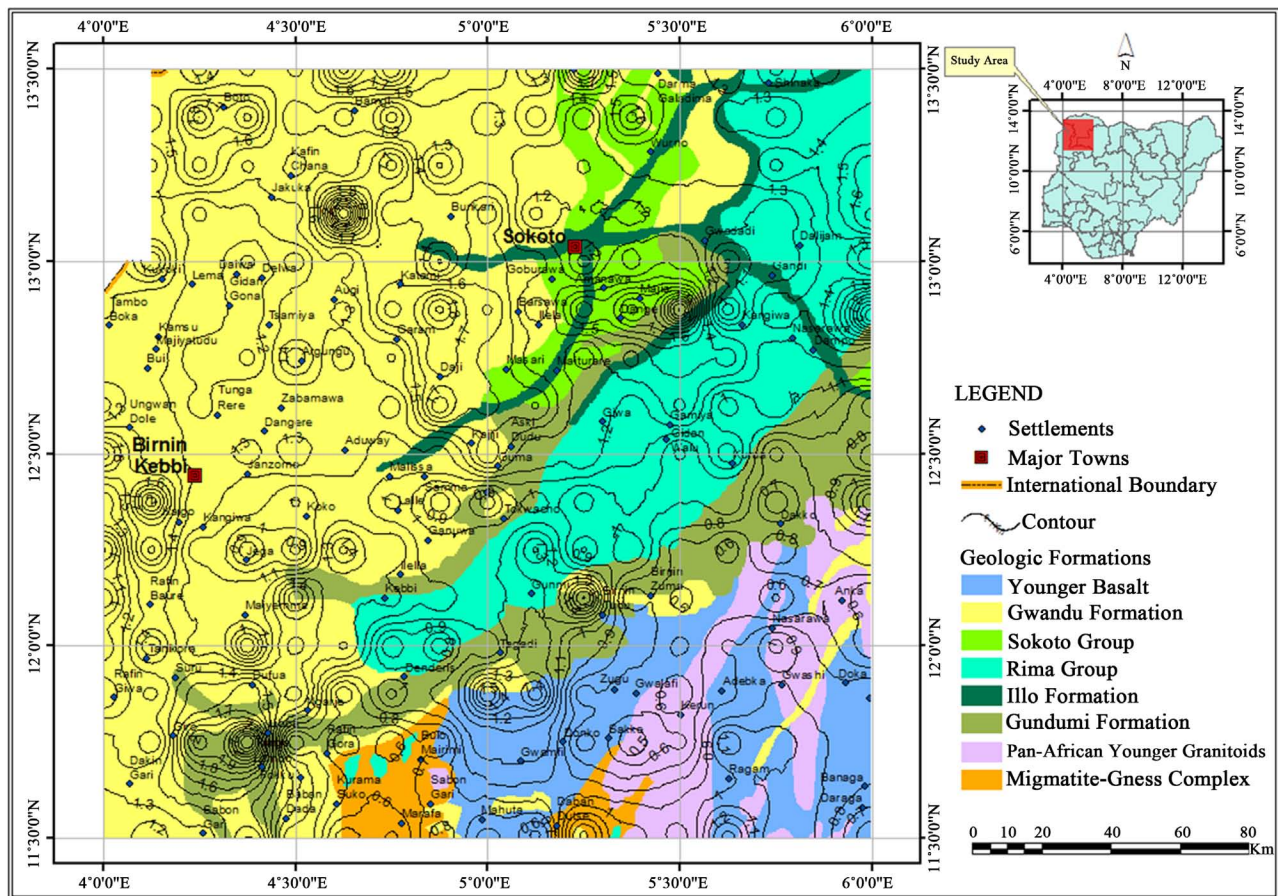


Figure 9. Deeper magnetic source depth (D1) super imposed on the Geologic Map of the study area.

3.2. Discussion

From the spectral analysis (**Figure 7**) various depths of D1, the summary of the result of the depths is presented in **Table 1**. A careful observation of the D1 map revealed Sub-Basins based on the various depths that were observed in the area. These depths are similar to ones obtained by [10] and [4]. The coloured areas on **Figure 7** are regarded as sub-basins because of their depth and thus high sediment thickness from 1.5 km and above. These are the possible potential areas for further hydrocarbon exploration. Though the result of the shallow Magnetic source depth (D2) shows that the basin is shallow with few identified areas of considerable depth indicating probable near surface igneous intrusions in the basin [10].

The major sub-basins identified include: sub-basin 1, with an approximate width of 43 km and length of 71 km; sub-basin 2, with an approximate width of 29 km and length of 31 km; sub-basin 3, with an approximate width of 20 km and length of 41 km; sub-basin 4, approximately 32 km in width and 39 km in length; sub-basin 5, with an approximate width of 19 km and length of 45 km; sub-basin 8, with an approximate width of 7 km and length of 40 km.

The result of the contoured deeper magnetic source depth (D1) was super imposed on the geologic map (**Figure 9**) to further observe the relationship of

the sediments thickness and geology of the area. This shows that the sediment over burden are of shallow depth in the basement compared to the sedimentary area. Most of the areas with high sediment thickness were observed on the Gwandu Formation. The shales of Dange, Kalambaina and Dukamaje Formations could be the source rocks, while grits and sandstones of Taloka and Wurno Formations could serve as the reservoir rock.

4. Conclusions and Recommendations

4.1. Conclusions

The following conclusions can be drawn from this study:

- 1) Spectral analysis indicates that the basin is characterized by shallow and deeper sediments thickness.
- 2) Areas with shallow thickness of sediments, could not allow thermal maturation of the sediments, since temperature increase with depth. Depth of 2 km and above has a temperature range of 60°C and above. The oil window according to [1] varies between 60°C and 120°C, above the temperature of 120°C the oil may be thermally cracked to gas, and below 60°C, it will form kerogen. Therefore areas with sediment thickness from 2 km and above could be good potential sites for hydrocarbon exploration.

4.2. Recommendations

The study area if given much attention, will add to the economic growth of Nigeria based on the hydrocarbon potentials revealed by this study. Therefore the use of other geophysical methods such as seismic and well logging is highly useful.

Acknowledgements

The author is grateful to the Nigerian Geological Survey Agency (NGSA), for releasing the High Resolution Digital Aeromagnetic data at a subsidized rate and Adamawa State University, Mubi Nigeria, for granting the author a study fellowship.

References

- [1] Nwanko, L.I. (2007) Spectral Evaluation of Aeromagnetic Anomaly Map for Geothermal Exploration in Part of Nupe Basin, West Central Nigeria. PhD Thesis, University of Ilorin, Ilorin.
- [2] Reynolds, J.M. (1990) An Introduction to Applied and Environmental Geophysics. John Wiley and Sons Limited, Hoboken, 116-207.
- [3] Abdulsalam, N.N., Nasir, M.A. and Likason, K.O. (2011) Identification of Linear Features Using Continuation Filters over Koton Karfi Area from Aeromagnetic Data. *World Rural Observation*, **3**, 1-8.
- [4] Obaje, G.N., Aduku, M. and Yusuf, L. (2013) The Sokoto Basin of Northwestern Nigeria: A Preliminary Assessment of the Hydrocarbon Prospectivity. *Petroleum Technology Development Journal*, **3**, 66-80.

- [5] Digital Elevation Model (2006) Topographical Map of Latitude 11°30'N-13°30'N and Longitude 4°00'E-6°00'E.
- [6] Kogbe, C.A. (1976) Outline of the Geology of Illummeden Basin, Geology of Nigeria. Elizabethan Publishing Co., 331-338.
- [7] Affodile, M.E. (2002) Ground Water Study and Development in Nigeria. 2nd Edition, Mecon Geology and Eng., Services Ltd., Jos, 453 p.
- [8] Jones, B. (1948) Sedimentary Rocks of the Sokoto Province. Bulletin of the Geological Survey of Nigeria, Vol. 18, Kaduna, 79 p.
- [9] Parker, D.H., Fargher Carter, M.N. and Turner, O.C. (1964) Geological Map of Nigeria Series 1:250,000.
- [10] Bonde, D.S., Udensi, E.E. and Rai, J.K. (2014) Spectral Depth Analysis of Sokoto Basin. *Journal of Applied Physics*, **6**, 15-21.
- [11] Nigerian Geological Survey Agency, NGSA (2006) Geological Map of Latitude 11°30'-13°30' and Longitude 4°00' and 6°00'.
- [12] Nigeria Geological Survey Agency, NGSA (2010) High Resolution Aeromagnetic Data, (16 Sheets), Latitude 11°30'-13°30' and Longitude 4°00'-6°00'.
- [13] Udensi, E.E. (2001) Interpretation of Total Magnetic Field over the Nupe Basin and the Surrounding Basement Complex, Using Aeromagnetic Data. Unpublished PhD Thesis, Ahmadu Bello University, Zaria.
- [14] Oasis montaj 7.0.1 QX Geosoft Inc. Queens Quay Terminal, 207 Queens Quay West Suit 810.
- [15] Parker Gay, S. (1963) Standard Curves for Interpreting Magnetic Anomalies over Long Tabular Bodies. *Geophysics*, **28**, 161-200. <https://doi.org/10.1190/1.1439164>
- [16] Spector, A. and Grant, F.S. (1970) Statistical Models for Interpreting Aeromagnetic Data. *Geophysics*, **35**, 461-470. <https://doi.org/10.1190/1.1440092>
- [17] Hahn, A., Kind, E.G. and Mishara, D.C. (1976) Depth Estimation of Magnetic Sources by Means of Fourier Amplitude Spectra. *Geophysical Prospecting*, **24**, 287-308. <https://doi.org/10.1111/j.1365-2478.1976.tb00926.x>
- [18] Oppenheim, A.V. and Schafer, R.W. (1975) Digital Signal Processing Practice. Hall International Inc., 1227-1296.